

Simulations of computational fluid dynamics (CFD) for the prediction of fibre orientation in SFRSCC

*Aimar Orbe¹⁾, Jesús Cuadrado²⁾, Ramón Losada³⁾ and Eduardo Rojí²⁾

^{1), 2), 3)} *Construction Engineering Area, Dept. of Mechanical Engineering, Engineering Faculty of Bilbao, University of the Basque Country (UPV/EHU), 48013 Bilbao, Spain*
²⁾ *jesus.cuadrado@ehu.es*

ABSTRACT

The prediction of fibre orientation in Steel Fibre Reinforced Self-Compacting Concrete (SFRSCC) represents one of its most interesting challenges. Casting of a full-scale wall is analysed and quality control methods are compared with simulations of Computational Fluid Dynamics (CFD). The acceptability of the expected orientations and those determined by diverse testing procedures are presented. Gerris flow solver is adopted to solve Navier-Stokes equations in a multiphase simulation.

1. INTRODUCTION

The development of Steel Fibre Reinforced Concrete (SFRC) has leapt forward over the past decade. This concrete includes short, discrete, randomly distributed fibres that reinforce the concrete matrix. Its benefits, with regard to the increase of ductility, tensile strength, and crack bridging capability have already been widely tested. However, its applications are mainly restricted to pavements and tunnel linings (delaFuente2012).

Self-Compacting Concrete (SCC) has also been more widely used as the casting of durable concrete has become simpler (Okamura 2003). Even though it is necessary to increment cement content, in order to mix a more viscous paste, both labour and material costs are reduced, which makes its overall cost economically attractive.

Performance improves when both concrete technologies are merged to produce what is known as Steel Fibre Reinforced Self-Compacting Concrete (SFRSCC). The fibres alter an already complicated mix-design, although this is an issue that can be successfully resolved with satisfactory knowledge of the materials in use. The granulometry of aggregates must be adequate to provide sufficient viscous paste to achieve the necessary fluidity and segregation resistance. Although the SCC tends not to need very coarse aggregates (maximum size ~ 12 mm), the geometry of the slender and the long fibres is less suitable. The moisture content of gravel and especially sand,

¹⁾ Assistant Professor

²⁾ Associate Professor

³⁾ Professor

Note: Copied from the manuscript submitted to "Computers and Concrete, An International Journal" for presentation at ASEM13 Congress

can substantially modify the mix-design. Self-compactability is very sensitive to increased water content, provoking segregation of the mass.

The inherent difficulty of assessing fibre orientation and its distribution in hardened concrete is the main drawback to its wider use. Although the isotropic behaviour of SFRC has been reported in the literature, the synergy of SFRC and SCC can force fibre orientation in the direction of the flow (Stähli 2008). By doing so, planar orientations and, even more, remarkable unidirectional orientations can be achieved. However, to date, the prediction of fibre orientation is rather more conjecture than methodical engineering.

The research is at a stage now where it has to focus on the prediction of fibre orientation. Computational tools have the potential to reduce uncertainty. Several currents of research seek to achieve that goal, such as homogeneous fluid, discrete particles, and particles suspended in a medium, although each one has its advantages and disadvantages (Gram 2011).

This paper presents a case study of the casting of a large SFRSCC wall and the agreement between the expected and the real fibre orientations. Computational Fluid Dynamics (CFD) simulations are carried out for this prediction, while magnetic methods determine the actual amount and their orientation. In parallel, aspects regarding the suitability of fibres, mix-design, casting processes, testing methods (NDT or otherwise) and mechanical properties are also analysed. The results reported in this paper form part of a wider research project focused on the industrial applications of the material.

2. CASE STUDY

Using real rather than laboratory-scale specimens is considered necessary, in order to work with concrete movements that are sufficiently representative. Hence, a real-scale SFRSCC wall (3-meters high, 6-meters long and 0.15-meters thick) was cast (Orbe 2012). The casting process was pumped from a lower corner, allowing the concrete to flow across the formwork. The thickness was selected based on the standardized dimension of specimens for the following tests to be performed. They encompass compression, shear, double punching, bending, permeability and magnetic tests. For that purpose, 380 prismatic (150x150x600 mm) and cubic (150x150x150 cm) specimens were cut from the wall, according to Fig. 1. Its components and mix-design were adequately selected to satisfy key points relating to self-compactability, strength and durability.

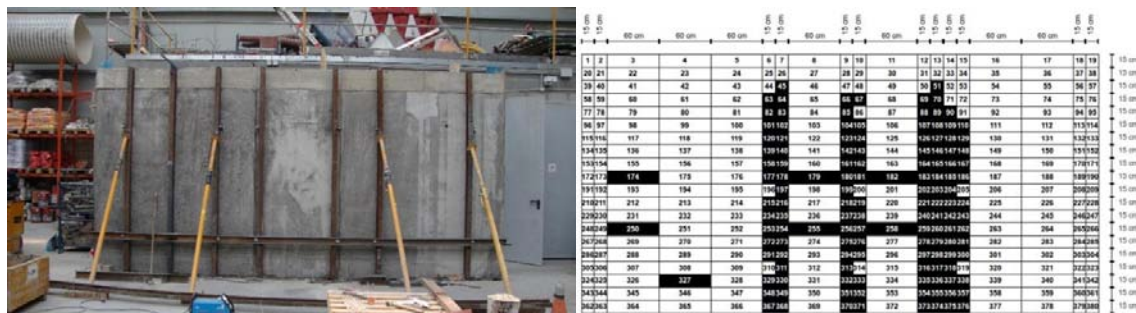


Fig. 1 Cast wall and cut scheme of specimens. Those in black have been measured by magnetic methods to determine fibre orientation and amount.

2.1 Metallic fibres

Hooked-end fibres were selected from among the several fibre types found on the market, as the hook provides the necessary anchorage to the concrete matrix, transferring tensile stress should cracks appear. The length and diameter are also basic aspects to define and the properties should be mid-way between the fresh and the hardened state.

Short lengths are more susceptible to slip from the matrix, but large ones make a robust and self-compacting mix-design complicated. Therefore, after suitable pull-out tests on individual fibres to verify the two preceding points, intermediate length fibres were chosen. The length and diameter of the selected fibres (HE 1/50) were 50 mm and 1 mm, respectively, as illustrated in Fig. 2.



Fig. 2 Tested steel fibres

2.2 Mix-design

The procedure of mixing is aimed to be used with close located materials. Based on previous experiences, adequate mix design is determined. Taking 350 kg/m³ of cement as minimum content, due to chemical attack by highly aggressive substances (EHE 2008), and 0.45 as its respective maximum water/cement ratio, proportions shown in Table 2 are determined. Even though cement amount could be considered high, aggressive exposures can lead to increase the minimum content to a closer value.

Table 1. Steel Fibre Reinforced Self-Compacting Concrete (SFRSCC) mix-design

Cement (CEM II 42,5R)	Sand (0/4)	Gravel (4/11)	Plasticizer	Superplasticizer	Steel Fibres (HE 1/50)	Water
434	1141	626	4.43	5.02	50	178

It is necessary to ensure the compactness of granular skeleton to obtain an adequate performance (durability and strength). So slender fibres are taken as new aggregates with an inadequate form factor, searching the proportions which lead to a lower porosity. Since there is no a method to predict the rheological behaviour of the mix, it is necessary to perform a series of characterization test. In this research V-funnel and slump flow tests have been carried out to optimize the admixtures amount. New generation of polycarboxylate ether-based superplasticizers (PCEs) have been employed as high range water reducers.

3. CONCRETE FLOW

Concrete motion was determined by solving the Navier-Stokes equations for a constant viscosity, as shown in Eq. (1), for which purpose the open source Gerris flow solver (Popinet 2003) was adopted. Considering an incompressible fluid, mass conservation must be guaranteed, according to Eq. (2).

$$\rho \left(\frac{\partial u}{\partial t} + u \nabla u \right) = \nabla \rho + \nabla(2\eta D) + \rho g \quad (1)$$

$$\nabla u = 0 \quad (2)$$

The Volume Of Fluid (VOF) technique was applied to track the free surface, which involves an adaptive mesh refinement, so that this gradient between concrete and air is simulated. The method provides accurate adaptation to changes in topology. Depending on the values of the injected tracer, both phases can be distinguished. Each volume fraction presents properties related to the tracer values, as indicated in Eq (3) to Eq (5). The tracer c adopts values from 0 to 1, for air and concrete, respectively. Intermediate values show the interface or gradient of the control volume.

$$\rho = \rho_{concrete} \cdot c + \rho_{air} \cdot (1 - c) \quad (3)$$

$$\mu = \mu_{concrete} \cdot c + \mu_{air} \cdot (1 - c) \quad (4)$$

$$\tau_0 = \tau_{0,concrete} \cdot c + \tau_{0,air} \cdot (1 - c) \quad (5)$$

Fluid movements are simulated assuming Bingham plastic behaviour (Fig. 4). Apparent viscosity is a basic input parameter, based on yield stress (τ_0) and plastic viscosity (μ). These values can be obtained from a rheometer, although (Hu 1995) has demonstrated that different devices show a diverse range of measured values. Another method involves the analysis of the slump flow test results: the final spread (D_f) and the time taken to pass over the 500 mm diameter circle (T_{50}). Yield stress is related to the maximum diameter the concrete will reach during the test, while viscosity mainly refers

to the speed at which it flows. SCC shows a lower yield stress value than vibrated concrete, due to its low resistance to flow, but its viscosity is higher as it contains more fine aggregates than vibrated concrete.

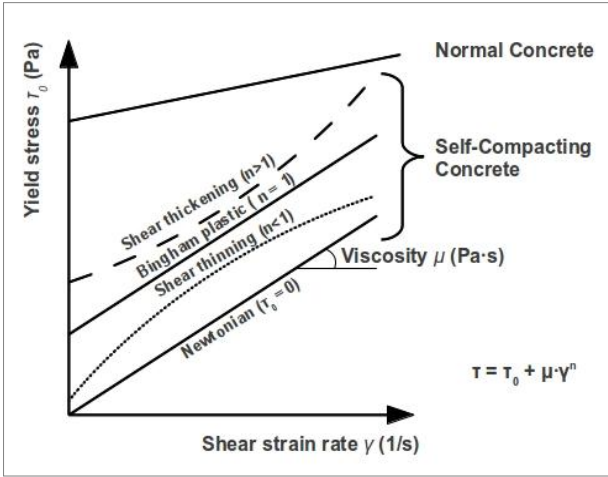


Fig. 4 Rheology models

Several slump flow tests were simulated in Gerris and compared with real slump tests and rheometer measurements (Zerbino 2009). The correlations made it possible to establish the input data (τ_0 and μ) needed from the proposed mix-design. Unlike studies done to date, the inclusion of a solid lifting cone in these simulations is notable. The mass only flows through the gap at the bottom of the cone, preventing horizontal movements at the top.

The parameters of the Bingham model were established from those simulations and with the slump flow test performed with the concrete that was pumped into the formwork. The final diameter (D_f) reached by the mass and the time it needed to arrive at a 500 mm diameter (T_{50}) were 710 mm and 1.9 s respectively. Those correlations suggest the concrete should be simulated as a Newtonian fluid, rather than a Bingham plastic, with a null yield stress ($\tau_0 = 0$ Pa) and low viscosity ($\mu = 63$ Pa·s). Some authors (Feys 2007) have argued that the Bingham plastic model is not the most appropriate with which to model concrete behaviour. The reason for this assertion lies in obtaining negative values of the yield stress for large slumps, which is physically impossible. This is the reason why a rather Newtonian model is adopted in this study. Even though the Bingham model underestimates the shear stress, other models such as Herschel-Bulkley (shear thickening) overestimate the yield stress. In this research, the Bingham model is preferred because its parameters have physical meaning and are easier to determine than those of the Herschel-Bulkley model.

4. CONFIGURATION OF THE SIMULATION MODEL

A complete model of the cast wall is represented in Fig. 5, in which the main

analysis centres on the 0.15 metre side boxes. These boxes are divided into 800 study units in accordance with the dimensions of the wall (length, height and thickness), although some of them are occupied by the pumping pipe. Solids are included to simulate the clamps arranged to tie both sides of the formwork, so as to consider the flow alteration that they could cause in the simulation.

The concrete is pumped in at the lower left corner of the formwork through a pipe and flows from left to right and from bottom to top, as it fills up. The upper face is open so that the air can escape without entrapment within the concrete.

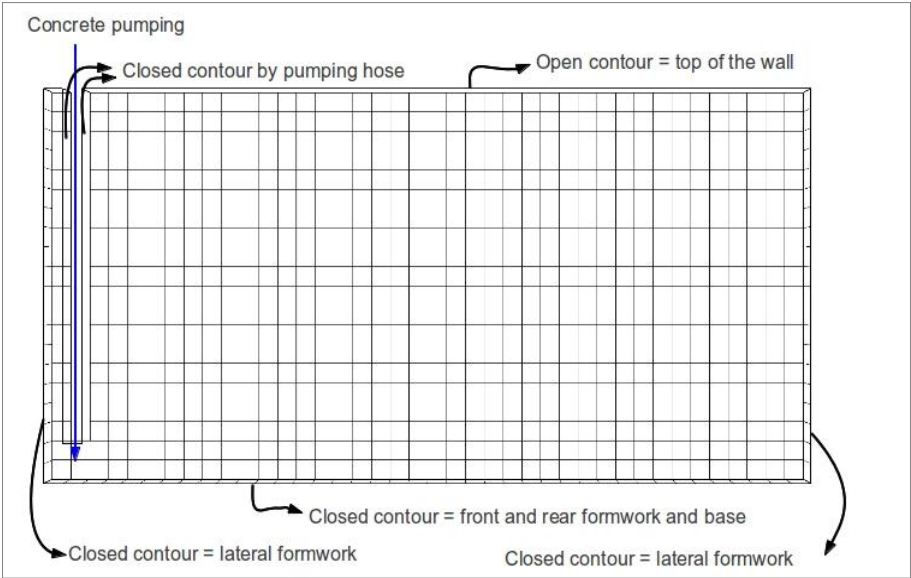


Fig. 5 Simulation model

The model implements a dynamic mesh refinement, focused on the interface and the high vorticity areas. This adaptive refinement promotes a better approach while reducing the computational cost, providing relevant information at selected points. These application criteria are then compared with the results of the magnetic method, for which 0.15 cm side cubic specimens are used. Therefore, the study boxes have the same dimension and are only refined up to 3 levels, when the concrete gradient passes through them and the vorticity inside is noteworthy. Fig. 6 shows the basic study unit referred to as a “box” and its different refinement types and levels. Geometrical discontinuities, such as clamps between lateral formworks, require static refinement throughout the simulation, to accommodate the mesh to such small holes. On the other hand, the refinement is also dynamically performed in some areas which need a closer approach, coarsening it later where the flow is stabilised. Parallel computing with multiple processors is used, which reduces the computational cost.

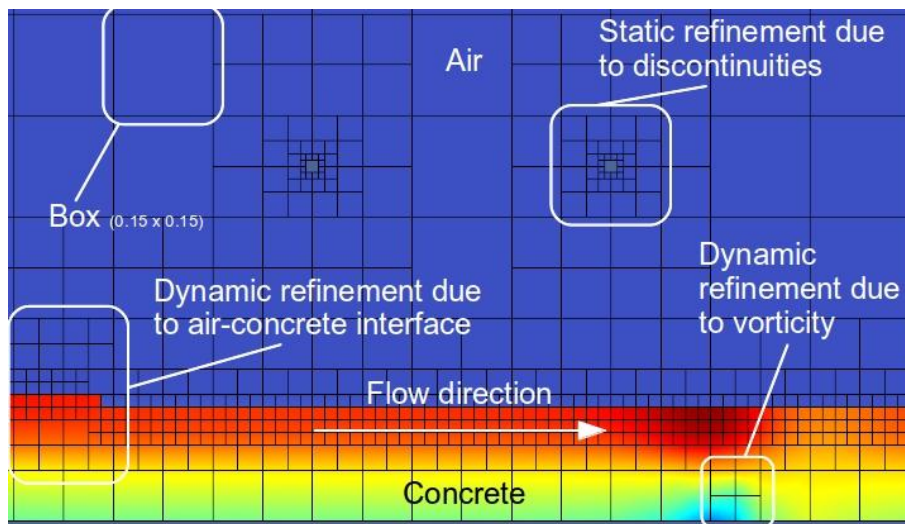


Fig. 6 Refinement criteria and levels

As a result, the position of the tracer, pressure and velocity fields of the two phases during the entire casting process were obtained for all the boxes at each time step. Since the study focuses on movement of the fresh concrete, the results of the gaseous phase are omitted.

Although the procedure and the results were initially different, the simulation was adapted to the specific case under analysis. There was still a slight difference between the casting process of the wall and its simulation, as the removal of the pumping equipment was not reflected in the latter. Pipe extraction would trigger a certain movement of the mass, especially in a vertical direction, that could change the local orientation of the fibres in the vicinity of the discharge point. However, as this was not considered very relevant for the mechanical behaviour of the whole wall, it was decided to limit the simulation to the concrete pumping process.

The simulation was performed in a manner that was consistent with the actual casting process, with the pumping pipe at the bottom of the formwork throughout the operation. This was not, however, the same as the previously established procedure, which determines a rate of ascent up the pipe as the concrete-air interface rises upwards. Nevertheless, casting procedures that were as real as possible were maintained in this study, as otherwise, the communication between agents is usually not as effective as expected. Consequently, the test replicates the conditions of placing concrete. The pumping rate is established, based on the time needed to complete the casting process. It took 8 minutes to fill the formwork with a volume of 2.7 m^3 , so $0.3375 \text{ m}^3/\text{min}$ were required. No-slip conditions were applied to the boundaries, therefore the speed of the concrete in contact with the formwork is null.

5. PREDICTION, MEASUREMENTS AND VALIDATION

During the simulation process, two velocity trends may be remarked. In the beginning, the concrete flows unimpeded along the length. As the pumped concrete

volume increases, boundary conditions slow down the mass that is located further away from the pumping point. The restructuring of the matrix, due to the common thixotropic behaviour of SCC, increases its shear strength. Therefore, newly pumped concrete has not got enough energy to displace the cement that has been previously poured and modifies the trend, rising to upper heights as Fig. 7 illustrates. The vertical component of the velocity vector in the proximity of the pumping pipe is noticeable to the detriment of the horizontal vector. The trend is reversed as the distance from the point of discharge increases and as the flow therefore stabilizes. However, the higher the level where the box is located, the greater the vertical/horizontal component ratio.

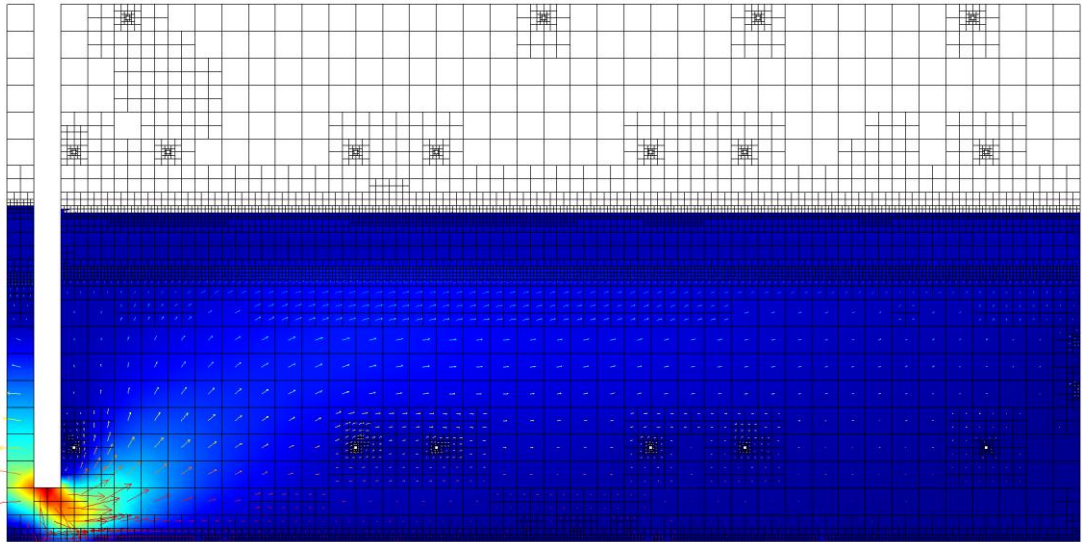


Fig. 7 Velocity field

All the velocity fields can be analysed for each individual box along the whole simulation. The tracer parameters are saved for each box in every time step. Fig. 8 shows the progression of both velocity components in box # 85 and # 294 during the simulation. For lower boxes, the horizontal velocity is predominant, although it tends to decrease rapidly along the simulation. For the upper boxes instead, both components are more similar and continue their displacement until the end of the pumping process. The concrete phase takes longer to reach those boxes, presenting a shorter impact on the simulation than lower ones.

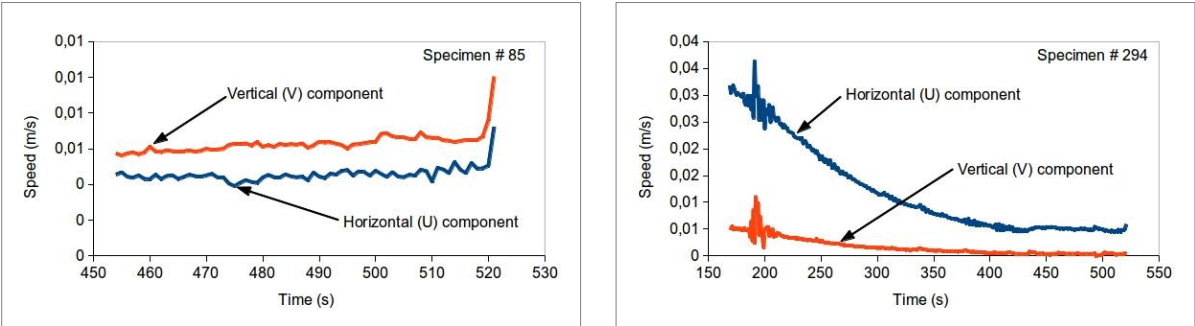


Fig. 8 Progress of speed fields for specimen #85 and #294.

These behaviours can be illustrated as an average orientation based on velocity component ratios. Thus, it is possible to compare simulation results with real orientation detected by NDT methods. Among the control techniques available, the most interesting one is the magnetic method. Its simplicity and the repeatability and reliability of the measurements made is proven (Torrents 2012).

The inductance of a given magnetic field, is altered when a ferromagnetic material is introduced. Three different coils were built and the proportionality of the measurements, based on their self-inductance, was verified. All the cubic specimens, 140 in total, were analysed through their three axes. Besides, 7 prismatic specimens were cut into four quarters, obtaining a further 28 cubic specimens, to which magnetic methods were applied. The orientation for each axis was determined by the inductance variation value in that direction and the average of the three axes is related to the fibre amount in the specimen. The X axis corresponds to the length of the wall, while the Z axis coincides with the height. The thickness or transversal direction of the wall is denoted on the Y axis, but as expected, fewer fibres are detected along that direction and they present less variation. Having such a thin wall prevents the mass from spatial flow, resulting in a two-dimensional flow as that adopted for the simulation. Fig. 9 shows a superposition of both data sets for the available specimens: those from the 2D simulation and the NDT testing. With the exception of some specimens, most of them show similar behaviour as expected. Note that cubic specimens are mainly analysed, because the set-up for the magnetic method fits the cubic ones best. Prismatic specimens can only be measured on the X axis, unless they are cut into quarters. This is done for 7 of them. The specimens from both sides were ignored, because a waterstop strip was attached to them and some nails arranged for fixing the wooden formwork altered the measurements. A slight segregation of fibres also occurred at the top due to some priming water in the pump, which meant that those specimens were also neglected.

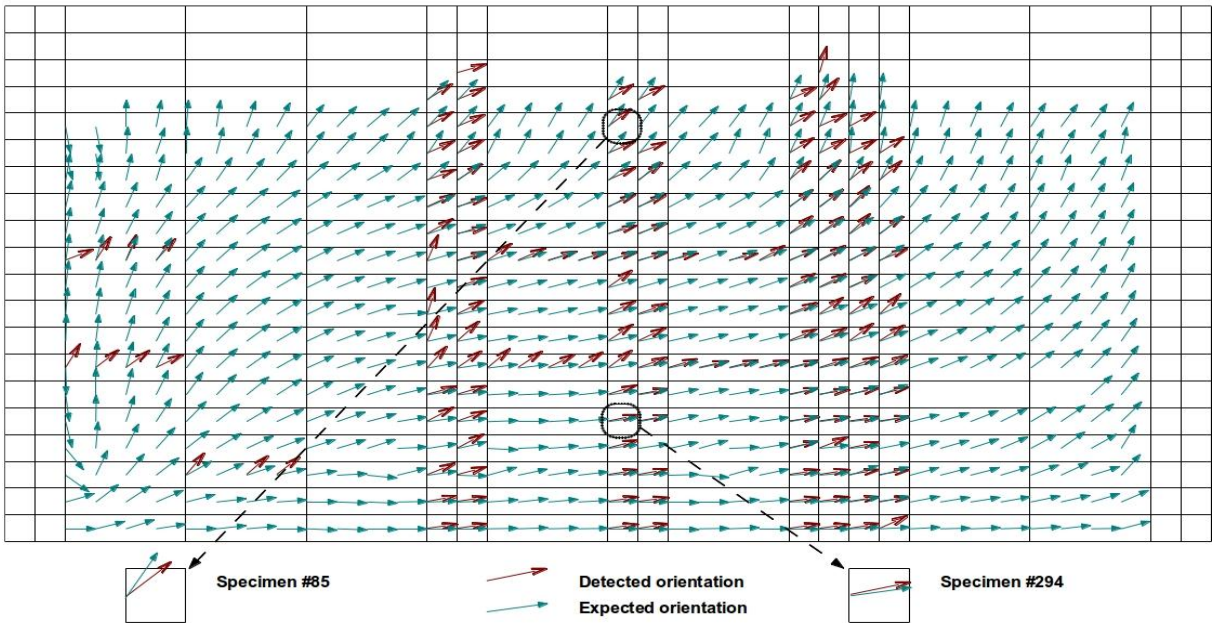


Fig. 9 Superposition of predicted orientations and detected ones

The lower side presented expected orientations, mainly on the X axis, while the upper sides tended to show a more influential vertical velocity component. This agrees with previous statements. Intermediate heights exhibit variable orientations depending of the distance from the pumping pipe and their proximity to the lateral formwork, which restrains the horizontal flow of the mass.

6. CONCLUSIONS

The study has presented the simulation and analysis of the casting procedure of a large 3 meter-high, 6 meter-long and 0.15 meter-thick wall. The quality control method provides good agreement with fibre density and orientation, although it needs to establish sufficiently reliable prediction techniques. CFD simulations provide a more accurate estimation of expected orientation patterns when compared with real ones.

SFRSCC flow is simulated as homogeneous Bingham fluid, even though in this case null yield stress is adopted, within a VOF numerical technique. Except for some particular areas, the predicted orientations fit the results of the magnetic tests quite well. This simple model can be improved with different rheological models and the incorporation of a restructuring rate for matching its thixotropic behaviour. Injecting Lagrangian particles in the fluid can also lead to approximate real fibre movement within the concrete.

Further research must be conducted on a parametric study of all the variables. Variations in thickness, length, height and pumping point should help establish an acceptable procedure to achieve the best performance.

ACKNOWLEDGEMENTS

The authors gratefully acknowledge the support obtained from the Spanish Ministry of Science and Innovation through MIVES IV ref: BIA 2010-20789-C04-04 grant. The first author is also grateful to ArcelorMittal - Wire Solutions and Financiera y Minera (Italcementi Group) for their participation in the mix-design phase.

REFERENCES

- delaFuente, A., Pujadas, P., Blanco, A. and Aguado, A. (2012) "Experiences in Barcelona with the use of fibres in segmental linings" *Tunn Undergr Sp Tech*, 27(1), 60-71.
- EHE (2008) "Instrucción de Hormigón Estructural" Comisión Permanente del Hormigón. Ministerio de Fomento.
- Gram, A. and Silfwerbrand, J. "Numerical simulation of fresh SCC flow: applications", *Mater. Struct.* 44(4), 805-813.
- Hu, Chong (1995) "Rheologie des betons fluides" L'Ecole Nationale des Ponts et Chaussées, Paris.
- Okamura, H. Ouchi, M. (2003) "Self-compacting concrete". *J. Adv. Concr. Technol.* 1(1),5-15
- Orbe, A. Cuadrado, J. Losada, R. Rojí,E. (2012), "Framework for the design and analysis of steel fibre reinforced self-compacting concrete", *Constr. Build. Mater.*, 35, 676-686.
- Popinet, S. (2003) "Gerris: A Tree-Based Adaptive Solver For The Incompressible

- Euler Equations In Complex Geometries”, *J. Comp. Phys.*, 190, 572-600.
- Stähli, P., Custer, R., Van Mier, J. (2008) “On flow properties, fibre distribution, fibre orientation and flexural behaviour of FRC” *Mater. Struct.* 41, 189-196
- Torrents, J.M., Blanco, A., Pujadas, P., Aguado, A., Juan-García, P. and Sánchez-Moragues, M.A. “Inductive method for assessing the amount and orientation of steel fibers in concrete”, *Mater. Struct.* 45, 1577-1592
- Zerbino, R., Barragán, B., García, T., Agulló, L., Gettu, R. (2009) “Workability tests and rheological parameters in self-compacting concrete” *Mater. Struct.* 42, 947-960.